Hindawi Publishing Corporation
Journal of Nanomaterials
Volume 2013, Article ID 542584, 9 pages
http://dx.doi.org/10.1155/2013/542584

Research Article

Development of Antibiotics Impregnated Nanosized Silver Phosphate-Doped Hydroxyapatite Bone Graft

Waraporn Suvannapruk, Faungchat Thammarakcharoen, Phetrung Phanpiriya, and Jintamai Suwanprateeb

National Metal and Materials Technology Center (MTEC), 114 Paholyothin Road, Klong 1, Klongluang, Pathumthani 12120, Thailand

Correspondence should be addressed to Jintamai Suwanprateeb; jintamai@mtec.or.th

Received 2 August 2013; Revised 2 October 2013; Accepted 2 October 2013

Academic Editor: In-Kyu Park

Nanosized Ag_3PO_4 loaded hydroxyapatite which was prepared by a novel low temperature phosphorization of 3D printed calcium sulfate dihydrate at the nominal silver concentration of 0.001 M and 0.005 M was impregnated by two antibiotics including gentamicin and vancomycin. Phase composition, microstructure, antibiotics loading, silver content, antimicrobial performance, and cytotoxic potential of the prepared samples were characterized. It was found that the fabricated sample consisted of hydroxyapatite as a main phase and spherical-shaped silver phosphate nanoparticles distributing within the cluster of hydroxyapatite crystals. Antibacterial activity of the samples against two bacterial strains (gram negative *P. aeruginosa* and gram positive *S. aureus*) was carried out. It was found that the combination of antibiotics and nanosized Ag_3PO_4 in hydroxyapatite could enhance the antibacterial performance of the samples by increasing the duration in which the materials exhibited antibacterial property and the size of the inhibition zone depending on the type of antibiotics and bacterial strains compared to those contained antibiotics or nanosilver phosphate alone. Cytotoxic potential against osteoblasts of antibiotics impregnated nanosilver phosphate hydroxyapatite was found to depend on the combination of antibiotics content, type of antibiotics, and nanosilver phosphate content.

1. Introduction

Hydroxyapatite is one of calcium phosphate family which is widely used for bone repairs and reconstruction due to its osteoconductive property. Recently, antibiotics impregnated hydroxyapatite which was prepared by a novel low temperature phosphorization route was developed for bone infection treatment by providing local, sustained, and high concentration of antimicrobial agents while also function as a restorable bone graft for new bone formation in the injured area [1, 2]. The advantages of this approach were that it minimized systemic complications which would expose patients to antibiotic levels that often would result in numerous toxic side effects, improved clinical efficacy, and eliminated the need for additional bone grafting. Furthermore, hydroxyapatite prepared by this low temperature process could resorb faster than typically used high temperature sintered hydroxyapatite [3–6] due to its low crystalline nanostructure which is close to that of bone.

Apart from antibiotics, silver ions were known to have inhibitory and antibacterial properties against a broad spectrum of bacterial strains while being relatively low toxic to human cells. Recently, silver nanoparticles have increasingly been used for infection treatment due to its unique properties resulting from the nanoscale features and the ability to rapidly release of several silver species which were seen to improve the treatment efficiency [7–9]. Silver phosphate (Ag_3PO_4) is one form of silver compounds that could be used as a silver source for antibacterial applications due to its advantages compared to other silver compounds including its low solubility in aqueous solutions, its high antibacterial efficiency, and its strong photocatalytic activity under visible light [10, 11]. Recently, we successfully applied a low temperature phosphorization process to *in situ* load nanosilver phosphate into hydroxyapatite structure in a single step which enhances its antibacterial property [12]. It was shown previously that the combination of nanosilver and antibiotics could enhance the antibacterial performance depending on the bacterial

strains, type of antibiotics, concentration of antibiotics, and nanosilver concentration [13–17]. However, no study on the effect of antibiotics and nanosilver that are incorporated into hydroxyapatite matrix on antibacterial activity has been studied. It is thought that the impregnation of antibiotics in nanosilver phosphate-doped hydroxyapatite could also provide the improvement in antibacterial performance of hydroxyapatite, but the mechanism and the effect might be different.

In this study, nanosilver phosphate-doped hydroxyapatite which was prepared by low temperature coconversion process was, thus, impregnated with two types of antibiotics including gentamicin and vancomycin. Materials properties and antibacterial performance including phase composition, microstructure, total drug loading, antibacterial activity, and cytotoxic potential of antibiotic impregnated nanosilver phosphate-doped hydroxyapatite sample were determined and compared to antibiotics impregnated only and nanosilver phosphate loaded only samples.

2. Materials and Method

2.1. Materials. Raw materials used in this study were calcium sulfate hemihydrate (Lafarge Prestia Co., Ltd, Thailand) and pregelatinized starch (Thaiwah Co., Ltd, Thailand). These materials were supplied in the form of powders and used without further sieving. Antibiotics used were gentamicin sulfate (T.P Drug Laboratories (1969) Co., Ltd) and vancomycin hydrochloride (CJ CheilJedang Corporation, Korea), abbreviated as CN and VC, respectively.

2.2. Sample Preparation. Calcium sulfate hemihydrate powders was mixed with pregelatinized starch powders using a mechanical blender and loaded into a three dimensional printing machine (Z400, Z Corporation) to print 7 mm in diameter spherical specimens. Solutions containing 1 M of disodium hydrogen phosphate (Fluka) and two concentration of silver nitrate (BDH) (0.001 and 0.005 M) were prepared, designated HA_001 and HA_005, respectively. Ammonium (BDH) was then added dropwise to the solution until clear solutions were obtained. The fabricated 3DP beads were then immersed in the solution and kept at 80°C for 24 hours to transform to nanosilver phosphate-doped hydroxyapatite by low temperature phosphorization reaction. Samples were then taken out, rinsed by distilled water, and oven-dried. They were then loaded with two types of antibiotics, using vacuum-assisted method similarly to previous studies [1, 2].

2.3. Characterization

2.3.1. Microstructure, Phase Composition and Total Silver Content. XRD characterization was carried out using X-ray diffractometer (JDX 3530, JEOL, Japan) with Co K-alpha radiation in the range of 10–80° 2θ with step angle of 0.02 degree. JCPDS files were used to identify the peaks of main compositions in sample. Microstructures of nanosilver phosphate loaded hydroxyapatite samples were examined using a transmission electron microscope (JEOL JEM-2010) and a scanning electron microscope (JSM-5410, JEOL, Japan). In the case of TEM analysis, all samples were grinded into powders and then dispersed onto continuous carbon film grids prior to observation. Total silver content in each sample was determined by acid digestion technique using an atomic absorption spectrometry (AAS) (Analyst 200, Perkin Elmer).

2.3.2. Total Antibiotic Loading. The total antibiotics concentration in the sample beads were determined by dissolving them in 2.4 M hydrochloric acid and analyzed by using UV-VIS spectrophotometer (Jasco V-530) in relation to the previously constructed calibration curve.

2.3.3. Minimum Inhibitory Concentration. Silver nitrate solution was employed to represent the silver ions that were expected to be released from nanosilver phosphate particles. Minimum Inhibitory Concentration (MIC) of silver nitrate and each antibiotic used against two bacterial strains (gram negative *P. aeruginosa* ATCC 27853 and gram positive *S. aureus* ATCC 25923) was determined by the broth macrodilution method. Bacterial inoculum was prepared by transferring 3–5 colonies of bacterial isolate from a fresh (18–24 h) nutrient agar plate to 5 mL of sterile nutrient broth (NB). It was incubated at 35°C ± 2°C for 4–6 h (become visibly turbid) and the culture was adjusted to a 0.5 McFarland standard ($\approx 1.5 \times 10^8$ CFU/mL). Tenfold serial dilution of the inoculum suspension was made by adding 1.0 mL of the inoculum suspension to 9.0 mL of NB to achieve 1.5×10^6 CFU/mL and gently mixing by the vortex mixture. Serial 2-fold dilution of the silver nitrate or antibiotic solution was made in the series of tubes and 0.5 mL of the prepared inoculum suspension was added to each tube and incubated at 35°C ± 2°C for 16–18 h. The growth of bacteria was shown as the visual turbidity and the MIC value was determined from the final silver nitrate or antibiotic concentration of the lowest concentration of nonturbid tube.

2.3.4. Antimicrobial Activity. All the samples were sterilized by ethylene oxide gas prior to the tests. Antimicrobial performance tests were carried out by modified agar diffusion assay against two bacterial strains (gram negative *P. aeruginosa* ATCC 27853 and gram positive *S. aureus* ATCC 25923). These two strains were selected to represent gram negative and gram positive strains that are commonly found in bone infection areas [18, 19]. Bacterial strains were inoculated on each agar plate. The sample beads were submerged in simulated body fluid (SBF) at 37°C for 15 days and the beads were withdrawn and placed in a new SBF at every 24 hours. Each eluate was placed in the bored holes in the agar plates and incubated at 37°C. Antibiotic assay was performed by measuring inhibition zone by a vernier caliper.

2.3.5. Cytotoxic Potential. All the samples were sterilized by ethylene oxide gas and incubated in 1 mL of DMEM (Biowhittaker) completed medium at 37°C. The eluates were drawn at 24, 48, and 72 hours with replenishment of a new medium after each eluate aspiration. This was devised to study and compare the effect of the releasing behavior

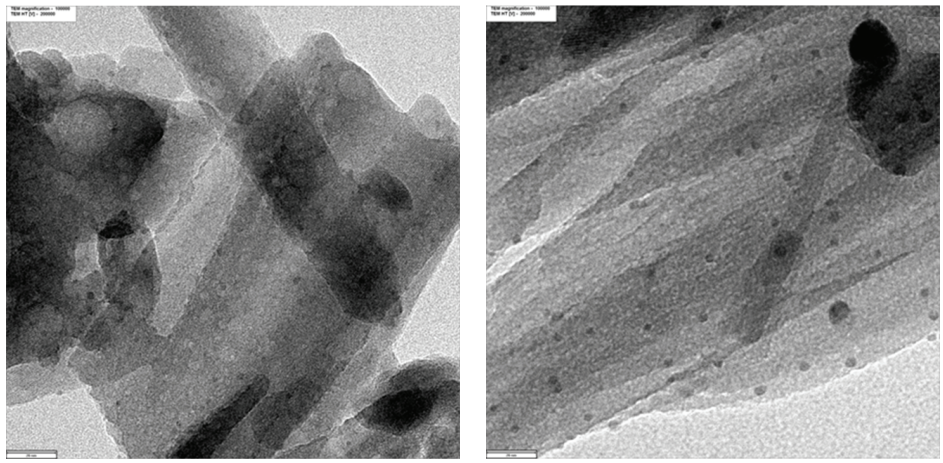

(a) (b)

Figure 1: TEM micrographs showing microstructure of nanosilver phosphate-doped hydroxyapatite. (a) HA001; (b) HA005. Scale bar = 20 nm.

of each sample on the cytotoxic potential at each period by the replenishment of a new medium after each eluate aspiration similar to the antimicrobial activity test. By this way, the media which contained released antibiotics and silver ions from the previous extraction period was discarded and the concentration of antibiotics or silver ions in the solution would be changed accordingly with extraction periods depending on the releasing characteristic. The elutes were then added to each tissue culture dish which contained 1×10^5 human osteoblast cells per one milliliter of DMEM medium and incubated for 24 hours. After incubation, 100 μL of 0.5 mg mL^{-1} MTT (Sigma-Aldrich) was added in each well and incubated for another 2 hours. Dimethyl sulfoxide was then added and transferred to a 96-well plate. Optical density was measured at the wavelength of 570 nm using a microplate reader (Easys Model UVM 340) to quantify the cell viability. Thermanox (Nunc) cover slip was used as negative control (NC) while polyurethane film containing 0.1% Zinc diethyldithiocarbamate (ZDEC): RM-A for ISO 10993 cytotoxicity testing (Hatano) was used as positive control (PC). Reagent control (RC) was the well which contained no samples. Hydroxyapatite sample (HA) which was fabricated by similar process, but without antibiotics or nanosilver phosphate loading, was also tested as a control sample.

2.3.6. Statistical Analysis. The differences in properties amongst samples were analyzed using an analysis of variance (ANOVA) and Tukey post hoc testing. A value of $P < 0.05$ was considered significant.

3. Results

3.1. Phase Composition and Microstructure. Figure 1 shows the typical microstructures of fabricated nanosilver phosphate-doped hydroxyapatite samples, HA_001 and HA_005. It was observed that both samples similarly comprised the nanosized crystals of hydroxyapatite with the distribution of spherical-shaped silver phosphate nanoparticles within the cluster. Particle sizes of silver phosphate particles in both samples were estimated from the images to be less than 5 nm. SEM images showed that as-fabricated nanosilver phosphate-doped hydroxyapatite sample was porous comprising numerous pores (Figures 2(a) and 2(b)). No significant difference in the microstructure between samples could be detected. Figure 3 shows the XRD pattern of sample fabricated by low temperature coconversion technique. HA_005 showed the characteristic peaks of hydroxyapatite and silver phosphate. HA_001 also showed the characteristic peaks of hydroxyapatite, but silver phosphate peaks were not clearly observed. In all samples, hydroxyapatite peaks were similarly broad while the silver phosphates peaks were sharp. Total silver content in each sample was determined by an atomic absorption technique and observed to be 0.09 and 0.42% for HA_001 and HA_005, respectively. After impregnation by antibiotic, the microstructure of the gentamicin impregnated samples appeared relatively unchanged (Figures 2(c) and 2(d)). In contrast, the surface of vancomycin impregnated samples was extensively coated by vancomycin (Figures 2(e) and 2(f)). This was owing to the greater gelation ability of vancomycin at high concentration compared to gentamicin.

3.2. Total Antibiotics Loading. Figure 4 shows the total antibiotics loading in the nanosilver phosphate-doped hydroxyapatite at different silver content. It could be seen that drug loading in pure hydroxyapatite samples was greater than those of nanosilver phosphate-doped samples for both type of antibiotics. In the case of gentamicin, the drug content in HA_CN_001 was not significantly different to HA_CN, but approximately twice greater than that of HA_CN_005. In contrast, the drug content in HA_VC_001 was lower than those of HA_VC and HA_VC_005.

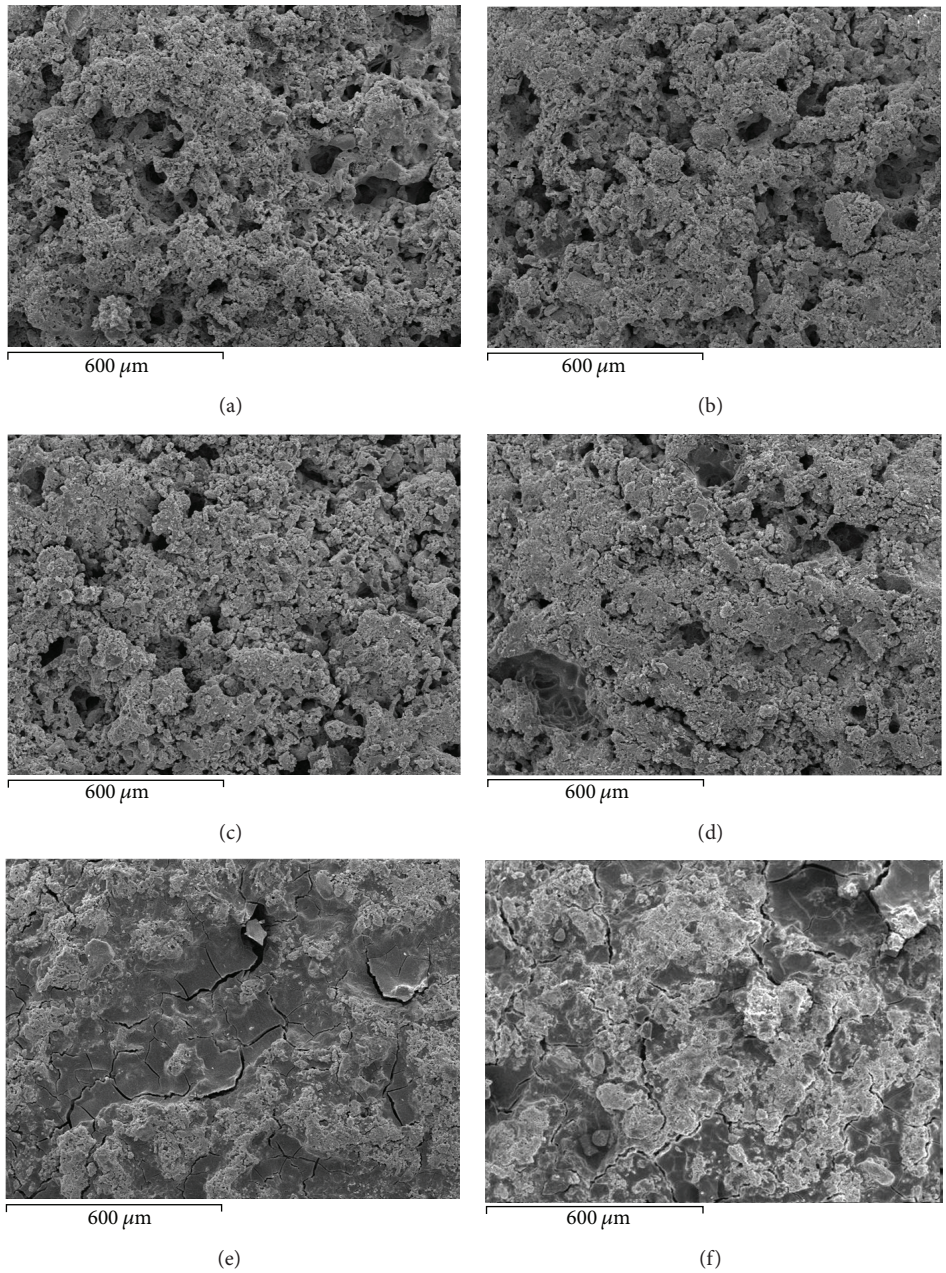

Figure 2: SEM images showing microstructure of nanosilver phosphate-doped hydroxyapatite and antibiotic impregnated nanosilver phosphate-doped hydroxyapatite samples: (a) HA_001; (b) HA_005; (c) HA_CN_001; (d) HA_CN_005; (e) HA_VC_001; (f) HA_VC_005. Scale bar = 600 μm.

3.3. Minimum Inhibition Concentration. Table 1 shows the MIC values for each antibiotic and silver nitrate (in the form of silver ions) against two bacterial strains. Gentamicin displayed the lowest MIC values, whereas vancomycin showed the highest values against *S. aureus*. In the case of *P. aeruginosa*, MIC value was not obtained for vancomycin since it is not active against gram negative bacteria. Silver ions showed lower MIC value than that of gentamicin.

3.4. Antibacterial Performance against P. aeruginosa. Figure 5 shows the antimicrobial performance of the samples against *P. aeruginosa*. In the case of vancomycin impregnated samples (Figure 5(a)), no inhibition zone was seen for HA_VC sample since vancomycin was known to be inactive against gram negative strains [20]. In contrast, vancomycin impregnated nanosilver phosphate samples (HA_VC_001 and HA_VC_005) showed inhibition zone. However, the sizes of the inhibition zone at the same period were observed to be similar to those of the hydroxyapatite samples containing similar content of nanosilver phosphate such as HA_VC_001 versus HA_001 or HA_VC_005 versus HA_005. In the case of gentamicin impregnated samples (Figure 5(b)), all gentamicin impregnated samples showed inhibition zone.

Table 1: Minimum inhibition concentration of the employed bacterial strains against each antibiotics and silver nitrate solution.

Antibiotics	Minimum inhibition concentration (g/mL)	
	P. aeruginosa ATCC 27853	*S. aureus* ATCC 25923
Vancomycin (VC)	No inhibition (>125)	0.975
Gentamicin (CN)	1.5625	0.0977
Ag^+ ($AgNO_3$)	0.3125	0.3125

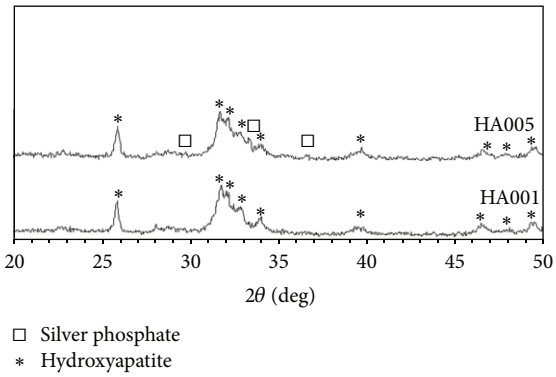

Figure 3: Phase composition of fabricated nanosilver phosphate-doped hydroxyapatite by low temperature phosphorization technique.

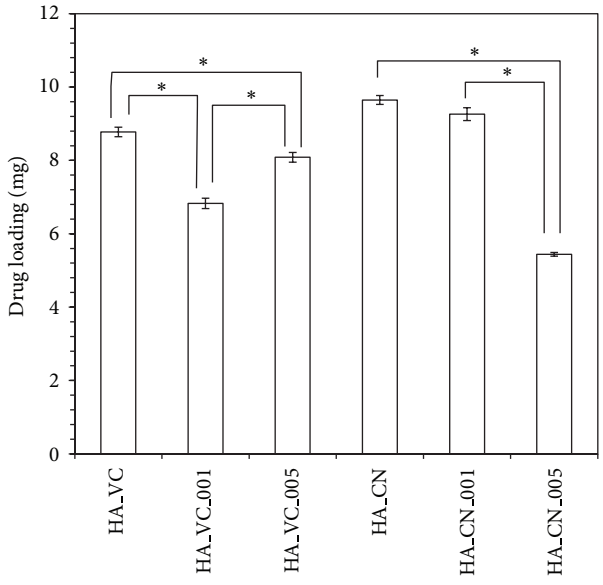

Figure 4: Total antibiotics content in the hydroxyapatite and nanosilver phosphate-doped hydroxyapatite samples (error bars = standard deviation, $n = 2$). $^*P < 0.05$.

The inhibition zones of samples containing both gentamicin and nanosilver phosphate were significantly greater than those of samples containing nanosilver phosphate alone and exhibited decreasing trends with extraction periods, whereas the inhibition zone size of nanosilver phosphate-doped samples was relatively constant throughout the extraction periods. HA_001, HA_VC_001 and HA_CN_001 samples displayed antibacterial duration for about 7 days while HA_005, HA_VC_005 and HA_CN_005 samples which contained large amount of nanosilver phosphate displayed longer antibacterial duration for about 15 days.

3.5. Antibacterial Performance against S. aureus. In the case of *S. aureus*, inhibition zones were seen for all samples. HA_001 showed limited antibacterial activity at day 2 extraction only while HA_005 displayed inhibition zone for only 5 days. The sizes of inhibition zone were also significantly lower than those of antibiotics impregnated nanosilver phosphate-doped samples. In the case of vancomycin impregnated samples (Figure 6(a)), HA_VC_005 showed the longest antibacterial duration followed by HA_VC and HA_VC_001, respectively. In contrast, both HA_CN_001 and HA_CN_005 showed about two times longer antibacterial duration than HA_CN sample (Figure 6(b)). The inhibition zones of samples containing both antibiotics and nanosilver phosphate displayed decreasing trends with extraction periods, whereas the inhibition zone size of nanosilver phosphate-doped samples was relatively constant throughout the extraction periods.

3.6. Cytotoxic Potential. Cytotoxic potential test (Figure 7) indicated that no cytotoxic potential at all extraction periods was observed for HA, HA_VC, and HA_VC_001 samples. However, HA_VC_005 sample showed cytotoxic potential (cell viability lower than 70%) even at day 3 extraction. In the case of gentamicin impregnated samples, HA_CN and HA_CN_005 samples displayed cytotoxic potential at day 1 extraction, whereas cytotoxic potential was observed until day 2 extraction for HA_CN_001 sample. In the case of nanosilver phosphate-doped hydroxyapatite alone, HA_001 sample displayed cytotoxic potential only at day 1 extraction, but no cytotoxic potential was observed at day 2 and longer extraction periods. HA_005 sample showed cytotoxic potential at all extraction periods, but cell viability tended to increase at longer extraction periods. The cell viability of the positive control sample remained low (less than 4%) at all extraction periods.

4. Discussion

A combination of a three dimensional printing technique and low temperature phosphorization process was previously shown to provide a simple mean to direct fabricate low crystalline nanostructure hydroxyapatite which is close to those of bone [21, 22]. This manufacturing route was subsequently developed to possess the antibacterial performance by employing either antibiotics impregnation or nanosilver compound incorporation [1, 2, 12, 23]. In this study, the

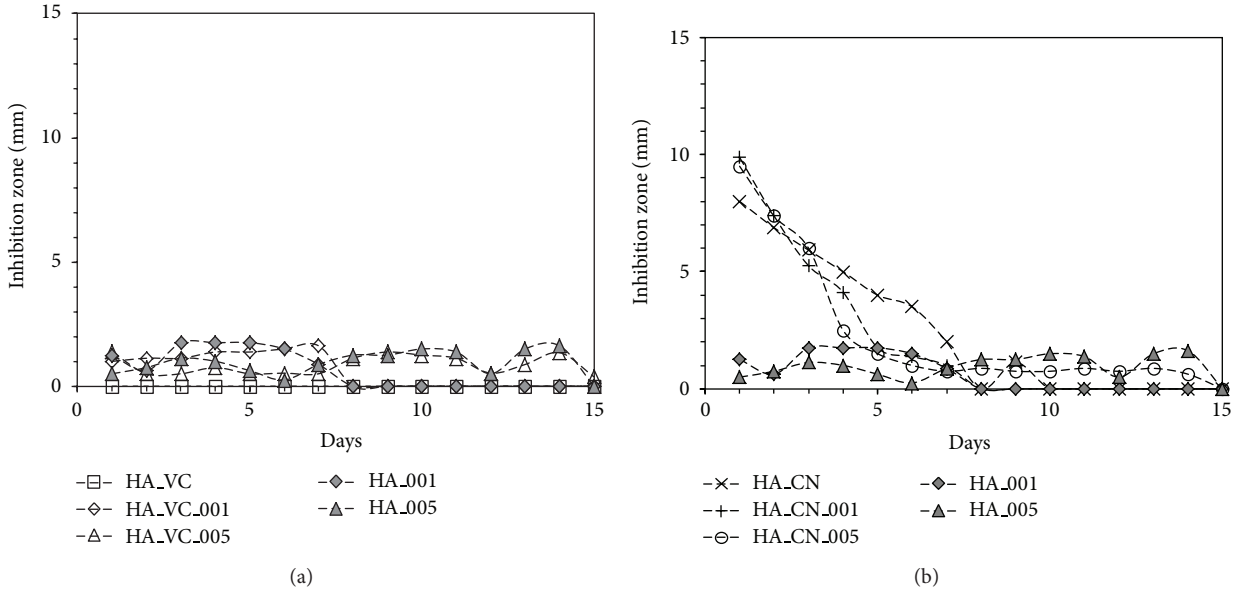

Figure 5: Antibacterial profile of VC (a) and CN (b) impregnated hydroxyapatites and nanosilver phosphate-doped hydroxyapatites against *P. aeruginosa* ($n = 2$).

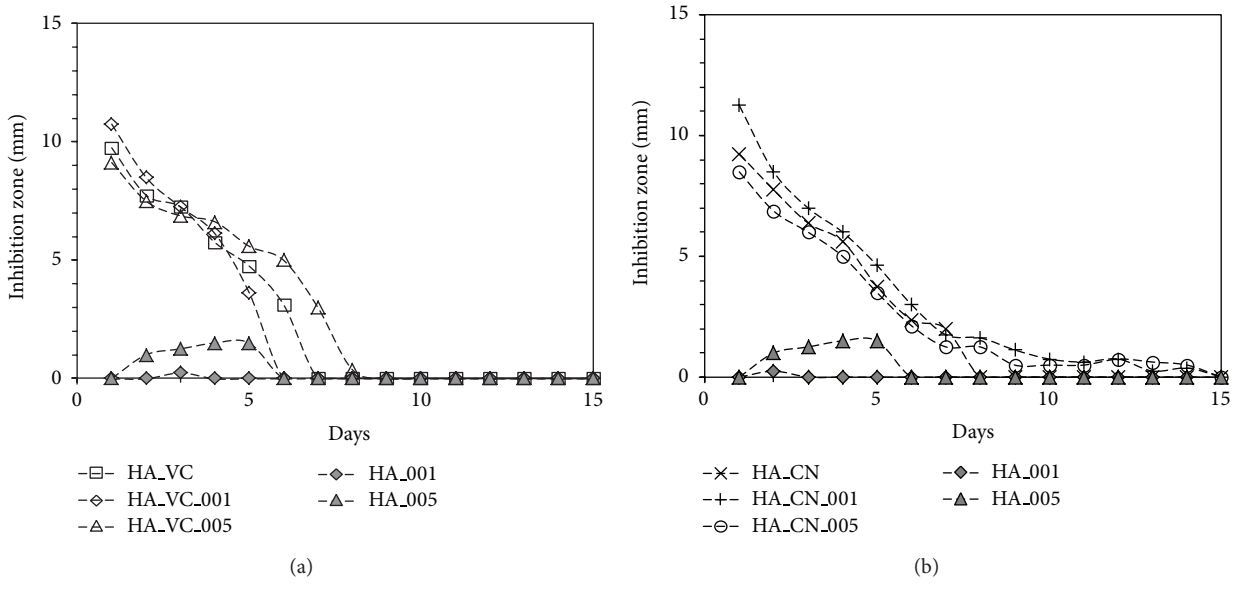

Figure 6: Antibacterial profile of VC (a) and CN (b) impregnated hydroxyapatites and nanosilver phosphate-doped hydroxyapatites against *S. aureus* ($n = 2$).

impregnation of antibiotics in nanosilver phosphate-doped hydroxyapatite was further developed to further provide the improvement in antibacterial performance of hydroxyapatite.

From XRD analysis, the characteristic peaks of nanosilver phosphate-doped hydroxyapatite were found to be broad and overlapped indicating the low crystallinity and nanosized crystals of the materials similar to those of bone mineral [24, 25]. Only silver phosphate peaks were observed without any other metallic silver bands. SEM and TEM analysis showed that the fabricated 3DP nanosilver phosphate-doped hydroxyapatite was highly porous and comprised the distribution of nanosized silver phosphate particles in the structure of nanosized hydroxyapatite crystals. After impregnation by antibiotics, difference in loading efficiency was observed. This difference in drug loading efficiency for both antibiotics could be related to the microstructure of the samples as a result of the fabrication process. The increase in degree of nanosilver phosphate incorporation in the sample tended to decrease the adsorption sites for the drugs in the samples due to the greater number and size of formed silver phosphate particles which could obstruct the diffusion of antibiotics solution into the samples. In

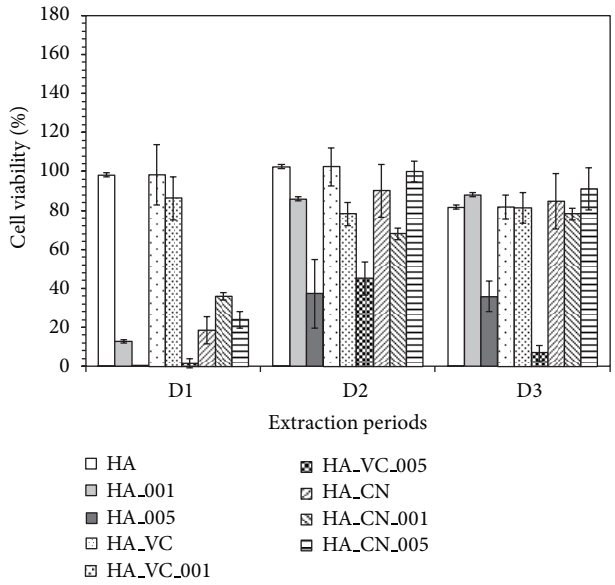

Figure 7: Cell viability of antibiotics impregnated nanosilver phosphate-doped hydroxyapatite samples using serial extraction technique (error bars = standard deviation, $n = 3$).

the case of vancomycin impregnated samples, the reincrease in antibiotics content in HA_VC_005 was noted. It was thought that this might be related to the greater gelling tendency of vancomycin on the sample surface than that of gentamicin. However, further investigation is needed to clarify this observation.

In term of antibacterial activity, no enhancement was observed from the combination of nanosilver phosphate and vancomycin against *P. aeruginosa*. However, some improvement in antibacterial duration for HA_VC_005 (7 days) when testing against *S. aureus* compared to HA_VC (6 days) or HA_005 (5 days) was noted. The combination of nanosilver phosphate and gentamicin seemed to give greater enhancement in antibacterial activity than vancomycin. This is possible due to the greater spectrum of activity, lower molar mass and lower minimum inhibitory concentration (MIC) of gentamicin [26]. MIC determination in Table 1 also confirmed that vancomycin has higher MIC values than both gentamicin and silver ions. In the case of *P. aeruginosa*, 21% and 814% increase in inhibition zone size at day 1 of both gentamicin impregnated nanosilver phosphate-doped samples (9.5–9.87 mm) compared to HA_CN (8 mm) and nanosilver phosphate-doped samples alone (0.87–1.25 mm), respectively, was observed. However, no improvement in antibacterial duration was observed. This improvement was thought to be the additional effect since the increase in the inhibition zone size was resulted from the sum of those of HA_CN and HA_001 or HA_005 samples. In the case of *S. aureus*, the enhancement in both initial inhibition zone size at day 1 and the antibacterial duration was seen for HA_CN_001, but not for HA_CN_005. A 22% increase in inhibition zone size at day 1 of HA_CN_001 (11.25 mm) compared to HA_CN (9.25 mm) was observed. The antibacterial duration increased from 7 days for HA_CN to 14 days for HA_CN_001. Therefore, the synergic effect resulting from the combination of gentamicin and nanosilver phosphate in HA_CN_001 was observed against *S. aureus*. The absence in enhancement of HA_CN_005 was thought to be due to its low gentamicin loading (Figure 4) which might be not sufficient to produce an improvement when combined with nanosilver phosphate. The antibacterial activity of nanosilver particles was generally attributed to its small size that could attach or penetrate the cell membrane of bacteria and disrupt the integrity of bacterial membrane [27, 28]. The possible mechanism of synergic antibacterial effect of nanosilver particles and antibiotics combination was hypothesized to be due to the binding of drug molecules onto the nanosilver which increasing the destruction and penetration into the cell wall of bacteria [16, 17]. However, in this study, nanosilver phosphate particles were incorporated into hydroxyapatite structure and could not attach and penetrate the cell membrane by themselves but only release silver ions to produce the antibacterial activity [27]. Therefore, the degree of bactericidal performance of nanosilver phosphate-doped hydroxyapatite was expected to be different from that of nanosilver phosphate particles. In this case, silver ions which were released from nanosilver phosphate-doped hydroxyapatite would prevent the DNA of bacteria from unwinding [17]. This would result in the difference in antibacterial activity enhancement caused by antibiotics impregnated nanosilver phosphate-doped hydroxyapatite as prepared in this study and the direct combination of nanoparticles and antibiotics as reported previously [13–17].

Cytotoxic potential of antibiotics impregnated samples and nanosilver phosphate-doped samples alone could be related to the amount of released silver and type of antibiotics. It was reported previously that vancomycin was less toxic to osteoblasts than gentamicin and required greater concentration to induce cytotoxicity [29, 30]. Therefore, HA_VC was less cytotoxic than HA_CN and HA_001 was less cytotoxic than HA_005. When the extraction periods increased, lower concentrations of both antibiotics and silver were released from the samples so the level of cytotoxic of the samples diminished with increasing numbers of extraction periods [31–33]. In the case of samples containing both nanosilver phosphate and antibiotics, HA_VC_005 samples showed cytotoxic potential even at day 3, whereas HA_VC and HA_VC_001 did not showed cytotoxic at all periods. This could be related to the cytotoxic potential of silver ions that was released from HA_005 samples which also showed cytotoxic potential at all periods. In the case of HA_VC_001, the noncytotoxic potential was possibly due to the lower level of released silver ions and the non-cytotoxic potential of vancomycin. In the case of gentamicin impregnated nanosilver phosphate-doped hydroxyapatite, HA_CN_001 showed the lower cell viability than HA_CN and HA_CN_005. One might expect that HA_CN_005 would show the greatest cytotoxic potential since it contained greater amount of silver phosphate similarly to that of HA_VC_005 sample. Unlike vancomycin, gentamicin was observed to be cytotoxic to osteoblasts. Thus, the content of gentamicin in the samples that could be released and resulted in cytotoxic

potential should also be taken into account. It was found that the gentamicin loading in HA_CN_001 was similar to that of HA_CN while that of HA_CN_005 was about twice lower (Figure 4). Therefore, the greater cytotoxic potential of HA_CN_001 was thought to be due to the combination of high content of gentamicin and nanosilver phosphate compared to the cytotoxic potential of gentamicin only in HA_CN and lower gentamicin content and higher silver phosphate content in HA_CN_005.

5. Conclusion

The combined use of nanosilver phosphate and antibiotics could enhance the antibacterial performance of the hydroxyapatite samples. Synergic enhancement was found for gentamicin impregnated nanosilver phosphate-doped hydroxyapatite against *S. aureus*, but additive effect was observed against *P. aeruginosa*. Limited enhancement was observed for vancomycin impregnated nanosilver phosphate-doped hydroxyapatite against *S. aureus,* but no improvement was seen against *P. aeruginosa.* These behaviors were related to the antibiotics and nanosilver phosphate content in the samples, type of antibiotics used, and bacterial strains tested.

Conflict of Interests

The authors declare that there is no conflict of interests regarding the publication of this paper.

Acknowledgments

Lafarge Prestia Co., Ltd. is thanked for the supply of calcium sulfate and Thaiwah Co., Ltd, Thailand, for the supply of pregelatinized starch. Cluster and Program Management Office, National Science and Technology Development Agency is acknowledged for financial support. W. Chokevivat (MTEC) was thanked for cytotoxic potential study.

References

[1] F. Thammarakcharoen and J. Suwanprateeb, "The effect of bead size on drug loading and releasing characteristic of antibiotic loaded 3DP calcium phosphate bead," in *Proceedings of the Pure and Applied Chemistry International Conference*, pp. 473–476, 2011.

[2] P. Phanphiriya, F. Thammarakcharoen, W. Chokevivat, and J. Suwanprateeb, "Antimicrobial performance and cytotoxicity of antibiotics impregnated hydroxyapatite for osteomyelitis treatment," *Advanced Materials Research*, vol. 506, pp. 513–516, 2012.

[3] Y. Shinto, A. Uchida, F. Korkusuz, N. Araki, and K. Ono, "Calcium hydroxyapatite ceramic used as a delivery system for antibiotics," *Journal of Bone and Joint Surgery B*, vol. 74, no. 4, pp. 600–604, 1992.

[4] Y. Yamashita, A. Uchida, T. Yamakawa, Y. Shinto, N. Araki, and K. Kato, "Treatment of chronic osteomyelitis using calcium hydroxyapatite ceramic implants impregnated with antibiotic," *International Orthopaedics*, vol. 22, no. 4, pp. 247–251, 1998.

[5] A. Ślósarczyk, J. Szymura-Oleksiak, and B. Mycek, "The kinetics of pentoxifylline release from drug-loaded hydroxyapatite implants," *Biomaterials*, vol. 21, no. 12, pp. 1215–1221, 2000.

[6] F. Chai, J.-C. Hornez, N. Blanchemain, C. Neut, M. Descamps, and H. F. Hildebrand, "Antibacterial activation of hydroxyapatite (HA) with controlled porosity by different antibiotics," *Biomolecular Engineering*, vol. 24, no. 5, pp. 510–514, 2007.

[7] C. Marambio-Jones and E. M. V. Hoek, "A review of the antibacterial effects of silver nanomaterials and potential implications for human health and the environment," *Journal of Nanoparticle Research*, vol. 12, no. 5, pp. 1531–1551, 2010.

[8] S. Sarkar, A. D. Jana, S. K. Samanta, and G. Mostafa, "Facile synthesis of silver nano particles with highly efficient antimicrobial property," *Polyhedron*, vol. 26, no. 15, pp. 4419–4426, 2007.

[9] Y. Li, L. Li, J. Li et al., "Antibacterial properties of nanosilver PLLA fibrous membranes," *Journal of Nanomaterials*, vol. 2009, Article ID 168041, 5 pages, 2009.

[10] C.-T. Dinh, T.-D. Nguyen, F. Kleitz, and T.-O. Do, "Large-scale synthesis of uniform silver orthophosphate colloidal nanocrystals exhibiting high visible light photocatalytic activity," *Chemical Communications*, vol. 47, no. 27, pp. 7797–7799, 2011.

[11] J. J. Buckley, A. F. Lee, L. Olivi, and K. Wilson, "Hydroxyapatite supported antibacterial Ag_3PO_4 nanoparticles," *Journal of Materials Chemistry*, vol. 20, no. 37, pp. 8056–8063, 2010.

[12] J. Suwanprateeb, F. Thammarakcharoen, K. Wasoontararat, W. Chokevivat, and P. Phanphiriya, "Preparation and characterization of nanosized silver phosphate loaded hydroxyapatite by single step co-conversion process," *Materials Science and Engineering C*, vol. 32, pp. 2122–2128, 2012.

[13] K. I. Wolska, K. Grzes, and A. Kurek, "Synergy between novel antimicrobials and conventional antibiotics or bacteriocins," *Polish Journal of Microbiology*, vol. 61, pp. 95–104, 2012.

[14] S. Ruden, K. Hilpert, M. Berditsch, P. Wadhwani, and A. S. Ulrich, "Synergistic interaction between silver nanoparticles and membrane-permeabilizing antimicrobial peptides," *Antimicrobial Agents and Chemotherapy*, vol. 53, no. 8, pp. 3538–3540, 2009.

[15] G. Geoprincy, P. Saravanan, N. Nagendra Gandhi, and S. Renganathan, "A novel approach for studying the combined antimicrobial effects of silver nanoparticles and antibiotics through agar over layer method and disk diffusion method," *Digest Journal of Nanomaterials and Biostructures*, vol. 6, no. 4, pp. 1557–1565, 2011.

[16] A. M. Fayaz, K. Balaji, M. Girilal, R. Yadav, P. T. Kalaichelvan, and R. Venketesan, "Biogenic synthesis of silver nanoparticles and their synergistic effect with antibiotics: a study against gram-positive and gram-negative bacteria," *Nanomedicine: Nanotechnology, Biology, and Medicine*, vol. 6, no. 1, pp. e103–e109, 2010.

[17] P. Li, J. Li, C. Wu, Q. Wu, and J. Li, "Synergistic antibacterial effects of β-lactam antibiotic combined with silver nanoparticles," *Nanotechnology*, vol. 16, no. 9, pp. 1912–1917, 2005.

[18] P. J. Carek, L. M. Dickerson, and J. L. Sack, "Diagnosis and management of osteomyelitis," *American Family Physician*, vol. 63, no. 12, pp. 2413–2420, 2001.

[19] P. D. P. Lew and P. F. A. Waldvogel, "Osteomyelitis," *The Lancet*, vol. 364, no. 9431, pp. 369–379, 2004.

[20] O. S. Kluin, H. C. van der Mei, H. J. Busscher, and D. Neut, "A surface-eroding antibiotic delivery system based on poly-(trimethylene carbonate)," *Biomaterials*, vol. 30, no. 27, pp. 4738–4742, 2009.

[21] J. Suwanprateeb, W. Suvannapruk, and K. Wasoontararat, "Low temperature preparation of calcium phosphate structure via phosphorization of 3D-printed calcium sulfate hemihydrate based material," *Journal of Materials Science: Materials in Medicine*, vol. 21, no. 2, pp. 419–429, 2010.

[22] J. Suwanprateeb, F. Thammarakcharoen, K. Wasoontararat, and W. Suvannapruk, "Influence of printing parameters on the transformation efficiency of 3D-printed plaster of paris to hydroxyapatite and its properties," *Rapid Prototyping Journal*, vol. 18, pp. 490–499, 2012.

[23] J. Suwanprateeb, F. Thammarakcharoen, K. Wasoontararat, W. Chokevivat, and P. Phanphiriya, "Single step preparation of nanosilver loaded calcium phosphate by low temperature co-conversion process," *Journal of Materials Science: Materials in Medicine*, vol. 23, pp. 2091–2100, 2012.

[24] R.-J. Chung, "Study of hydroxyapatite nano composites with photoluminescence properties," *Biomedical Engineering*, vol. 23, no. 2, pp. 107–112, 2011.

[25] F. Peters, K. Schwarz, and M. Epple, "The structure of bone studied with synchrotron X-ray diffraction, X-ray absorption spectroscopy and thermal analysis," *Thermochimica Acta*, vol. 361, no. 1-2, pp. 131–138, 2000.

[26] S. Alvarez, M. Jones, and S. L. Berk, "In vitro activity of fosfomycin, alone and in combination, against methicillin-resistant Staphylococcus aureus," *Antimicrobial Agents and Chemotherapy*, vol. 28, no. 5, pp. 689–690, 1985.

[27] J. R. Morones, J. L. Elechiguerra, A. Camacho et al., "The bactericidal effect of silver nanoparticles," *Nanotechnology*, vol. 16, no. 10, pp. 2346–2353, 2005.

[28] M. J. Hajipour, K. M. Fromm, A. A. Ashkarran et al., "Antibacterial properties of nanoparticles," *Trends in Biotechnology*, vol. 30, pp. 499–511, 2012.

[29] V. Antoci Jr., C. S. Adams, N. J. Hickok, I. M. Shapiro, and J. Parvizi, "Antibiotics for local delivery systems cause skeletal cell toxicity in vitro," *Clinical Orthopaedics and Related Research*, no. 462, pp. 200–206, 2007.

[30] C. R. Rathbone, J. D. Cross, K. V. Brown, C. K. Murray, and J. C. Wenke, "Effect of various concentrations of antibiotics on osteogenic cell viability and activity," *Journal of Orthopaedic Research*, vol. 29, no. 7, pp. 1070–1074, 2011.

[31] W. Chen, Y. Liu, H. S. Courtney et al., "In vitro anti-bacterial and biological properties of magnetron co-sputtered silver-containing hydroxyapatite coating," *Biomaterials*, vol. 27, no. 32, pp. 5512–5517, 2006.

[32] B. Singh, A. K. Dubey, S. Kumar, N. Saha, B. Basu, and R. Gupta, "In vitro biocompatibility and antimicrobial activity of wet chemically prepared $Ca_{10-x}Ag_x(PO_4)_6(OH)_2$ $(0.0 \leq x \leq 0.5)$ hydroxyapatites," *Materials Science and Engineering C*, vol. 31, no. 7, pp. 1320–1329, 2011.

[33] G. Gosheger, J. Hardes, H. Ahrens et al., "Silver-coated megaendoprostheses in a rabbit model—an analysis of the infection rate and toxicological side effects," *Biomaterials*, vol. 25, no. 24, pp. 5547–5556, 2004.